

Hybrid-fed shared aperture antenna array for X/K-band airborne synthetic aperture radar applications

Venkata Kishore Kothapudi¹  | Vijay Kumar² 

¹Department of Electronics and Communication Engineering, Center of Excellence-Advanced RF Microwave & Wireless Communications, Vignana's Foundation for Science, Technology, and Research (VFSTR), Guntur, Andhra Pradesh, India

²Department of Communication Engineering, School of Electronics Engineering, Vellore Institute of Technology (VIT), Vellore, Tamil Nadu, India

Correspondence

Vijay Kumar, Department of Communication Engineering, School of Electronics Engineering, Vellore Institute of Technology (VIT), Vellore, Tamil Nadu, India.

Email: kumarvijay@icee.org

Funding information

Science and Engineering Research Board, Grant/Award Number: No.SB/DGH-82/2014

Abstract

The design of X/K-band shared aperture antenna (SAA) single-linear polarized K-band, dual-polarized (linear/circular) X-band 36-elements (6×6) planar array antenna with high gain, and low cost for airborne synthetic aperture radar systems is presented. To reduce the complexity and size of the feed networks, the concept of series-feed centre-fed open stub array with Chebyshev amplitude distribution of −25 dB side-lobe levels (SLL) are employed for K-band design. Two typical frequencies, X-band and K-band of 9.65 and 21 GHz, are chosen (frequency ratio of 1:2.176) in this proposed SAA design on a single-layer printed circuit board. For K-band design, SLL can be controlled by Chebyshev distribution. The amplitude is controlled by the width of the individual patch in the linear array with left and right symmetries. A 50-Ω microstrip line with 0.7λ spacing is used in between the patches for the ±25° scan angle requirement. The measured results are consistent with the simulations and provide a matching impedance bandwidth of 10.36/1.45% at X/K-bands, respectively. The array also has a high aperture efficiency of more than 85%, SLL of (X/K-bands: −18.9/−25 dB), and gain of (X/K-bands: 24.2/17.4 dBi).

1 | INTRODUCTION

Airborne synthetic aperture radar (ASAR) systems are end-to-end multimode systems with concurrent capabilities and are intended for civil and military applications like tactical surveillance and target reconnaissance [1]. SAR has been very useful over a wide range of applications, including sea and ice monitoring, mining, oil pollution monitoring, oceanography, snow monitoring, and classification of Earth terrain [2–7].

The SIR-C/X SAR (operating with L/C/X-bands of weight around 3000 kg) on the American Space Shuttle Endeavour (ASSE), a high-resolution 3D imaging radar, acquired images first time throughout the world in 2000 [8]. It consists of three individual dual-polarized sub-arrays operating at L-, C-, and X-bands, respectively. This resulted in a large and bulky structure weighing over 3000 kg. Shared aperture antenna (SAA) (dual/multi-band) can be advantageous for SAR system design. An SAA compact design for L- and C-bands is proposed by Axness [9] to overcome the limitations of SAR antenna designs. More commonly, dual-band antenna design can be achieved either by two single-band elements or

one dual-band element or multilayer configuration based on microstrip patch antenna technology [10]. The use of two single-band elements (either single or multilayer) is always considered to be a more efficient antenna aperture than conventional designs with a high-frequency ratio of more than 2. In [11–15] perforated square patch antennas, dual-band arrays are designed by sharing the common aperture. In articles [16–20] for dual-band operations, the radiating elements with different resonant frequencies are interlaced. The placement of feeding networks is one of the most difficult tasks in these array designs, as each band and each polarization are usually excited separately to provide better isolation and cross-polarization levels (X-pol). For improved inter-band isolation, designing a feeding system for the frequency ratio <2 would be a much challenging task in SAA. Several studies have been made to provide differential feeding and corporate binary feed networks to enhance the isolation in multilayer antenna configuration to provide a gain of 6.9 and 21.4 dBi at lower and higher bands. A dual-band dual polarized (DBDP) SAA, Tx/Rx self-diplexing phased array with a frequency ratio 1.5:1 at K/Ka-band has been presented with a realized gain of 4.4 and 4.6 dBi by [21], which is less for SAR applications. The

This is an open access article under the terms of the Creative Commons Attribution License, which permits use, distribution and reproduction in any medium, provided the original work is properly cited.

© 2020 The Authors. *IET Microwaves, Antennas & Propagation* published by John Wiley & Sons Ltd on behalf of The Institution of Engineering and Technology.

bandwidth improvement in both L/X-bands has been achieved in [22] using stacked patches with a gain of 11.1/23.5 dBi at L- and X-bands, respectively. A concept of the Fabry–Perot resonant cavity as a metasurface was implemented for achieving a gain of 16.2/21.2 dBi at C/X-band SAA [23].

A DBDP SAA single layer with 4×4 array elements is implemented at X/Ku-band with an impedance bandwidth of 8.3% and 18.2%, but it provided a side-lobe level (SLL) of less than -9 and -10 dB at X- and Ku-bands, respectively [24]. A circularly polarized (CP) SAA of 2×2 elements (with gain 14.5 dBi) at C-band and 4×4 array (gain of 17.5 dBi) at X-band has been implemented with an SLL of less than -12.5 and -15 dB, respectively [25]. An SAA with Ku/K (tri-band resonance) planar antenna array with similar shaped radiation patterns is innovatively interleaved on the common aperture with a gain 11 and 14.4 dBi has been presented in [26]. An SAA with X/Ku/Ka (tri-band) planar antenna array with perforated, stacked, and slim crossed patches are innovatively interleaved on the common aperture has been presented in [27]. So far, there is no SAA combination with X/K-band that has been communicated with improved gain. Herein, we proposed a series-fed X/K-band SAA using single-layer technology to provide higher gain (24/17 dBi) and lower SLLs (-26 dB) for meeting the requirements of airborne synthetic aperture radar (ASAR).

This paper presents a dual-band single-layer SAA with dual polarization at X-band and single polarization at K-band SAA. In practical applications, the advantages of multiband operation in multifunctional radar systems have been verified [8]. To date, the majority of the work reported was focused on the multi-layer structure. The authors in [28] reported a design of DBDP series-fed S/X-band SAA with four groups of 2×2 planar arrays for X-band and a single dual-port S-band patch has been implemented which has an impedance bandwidth of 9.3% and 1.72% at both S/X-bands with the cross-band isolation more than 25 dB. The authors in [29] designed an X-band dual linear polarized 6-port 3×3 series-fed planar antenna array with good inter-port and intra-port isolation which we have adopted in this X/K-band SAA as a single group, and this will be the starting point for implementing X/K-band SAA with a single layer.

The works reported in [21–26,28,30] present SAA design, which have many advantages like (1) low cost and low profile (single-layer printed circuit board [PCB]); (2) efficient utilization of physical aperture; single-layer PCB features amplitude control with controlling the patch width, SLL reduction, array group segmentation, and gain enhancement (24 dBi/17 dBi at X/K-bands) (it's a drawback in multilayer SAA technology); (3) series-fed design to reduce the microstrip transmission line losses; (4) minimized aperture size $150 \text{ mm} \times 150 \text{ mm} \times 1.6 \text{ mm}$ (almost $250 \text{ mm} \times 250 \text{ mm} \times 15 \text{ mm}$ in multilayer SAA); (5) design provides four groups of X-band 3×3 series-fed arrays, one of the groups [29] can be used as TX and other can be used as Rx; and (6) passive phased array system. No need of an external digital attenuator and phase shifter for amplitude and phase control; 7) Inter-element spacing of 0.7 free space wavelengths

allows less number of elements with required directivity and beamwidth and provides a scanning capability of $\pm 25^\circ$ which allows grating lobe free scanning. All of these advantages make it ideal for the present SAA design. The specifications and design goals of this work are summarized in Table 1.

This paper is organized as follows. Section 2 presents the geometry of the SAA X/K-band array. Section 3 summarizes the results and discussions and the conclusion is followed in Section 4.

2 | SAA DESIGN SPECIFICATIONS

Table 1 shows the dual-polarized X-band and single-polarized SAA K-band specifications. For X- and K-band operations, the resonant frequency is 9.65 and 21 GHz, respectively. For both bands, the bandwidth must be 200 MHz. Dual/single linear polarizations (LPs) are expected in each band. Isolations between ports must exceed 25 dB. For all operations, the antenna must also have a low X-pol level of -25 dB. The choice of frequency and beam patterns has been guided by the specific airborne SAR applications.

2.1 | SAA design configuration

An SAA dual/single-polarized dual-band antenna with a high-frequency ratio of approximately 2.176 is to interlace two different arrays using a single layer in the common aperture. Figure 1 shows the proposed X/K-band SAA geometry. The SAA design consists of a single substrate. To utilize the common aperture, 3×3 array groups and series-fed amplitude-controlled patch array has been implemented. Square microstrip patches are utilized for X-band, and for K-band array elements are rectangular patches with variable width for controlling the amplitude. Both arrays are placed on the top of the substrate while keeping the isolation between the two

TABLE 1 X/K-band single-layer shared aperture antenna specifications

Operation bands	X-band	K-band
Centre frequency	9.65 GHz	21 GHz
Polarization	Dual-linear	Single
Impedance bandwidth	200 MHz	200 MHz
Antenna size	$150 \times 150 \times 1.6 \text{ mm}^3$	
Radiation efficiency	80%	80%
Gain	20 dBi	15 dBi
Cross-polarization	>25 dB	>25 dB
Isolation	>25 dB	>25 dB
Side-lobe level	-15 dB	-25 dB
Scan range	$\pm 25^\circ$	$\pm 25^\circ$
Inter-element spacing	0.7λ	0.7λ

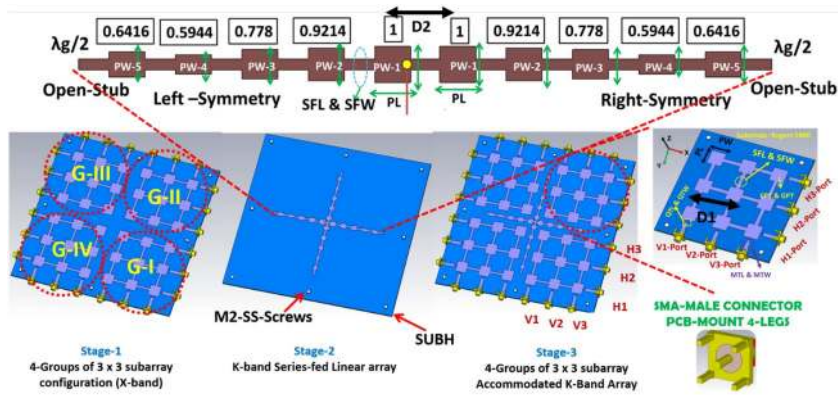
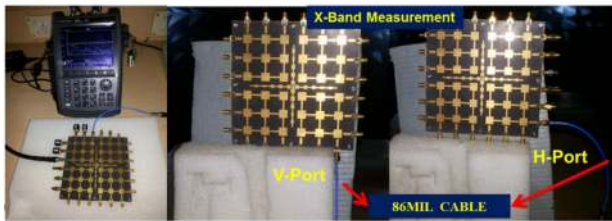


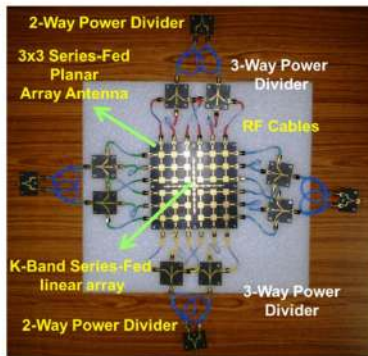
FIGURE 1 Geometry of X/K-band shared aperture antenna. $D1 = 22$ mm. $D2 = 10$ mm. $SUBH = 0.787$ mm

3

(a)



(b)



(c)

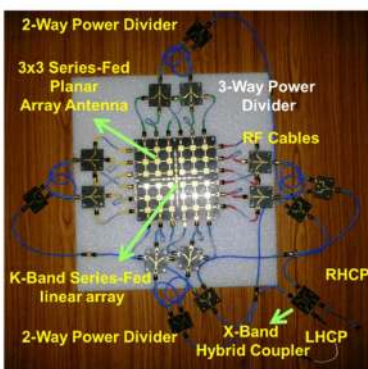


FIGURE 2 Proto-type of the X/K-band shared aperture antenna (SAA). (a) Measurement set-up. (b) Combined V-and H-ports with two-way and three-way power combiner/dividers for linear polarization. (c) V-port and H-port SAA X/K-band array with hybrid coupler for circular polarization (CP) (left-hand CP/right-hand CP)

TABLE 2 Parameters of X/K-band single-layer shared aperture antenna

Parameter	Description	Value (mm)
X-band		
PL	Patch length	10
PW	Patch width	10
QTL	Quarter wave transformer length	2
QTW	Quarter wave transformer width	0.28
MTL	Length of the matching transformer	10.25
MTW	Width of the matching transformer	2.46
SFL	Length of the series-fed line	22
SFW	Width of the series-fed line	1.9
SUBL	Length of the substrate	150
SUBW	Width of the substrate	150
SUBH	Height of the substrate	0.787
K-band		
PL	Length of the patch	5
PW-1	Width of the centre patch	5
PW-2	Width of the patch-2	4.6
PW-3	Width of the patch-3	4.15
PW-4	Width of the patch-4	2.75
PW-5	Width of the patch-5	3.5
SFL	Series-fed line length	4.28
SFW	Series-feed line width	1.5

bands minimum. The two-way and three-way power dividers have been used for combining the X-band groups to enhance the gain and narrowing the beamwidth.

For grating lobe-free scanning, the distance between the two elements for X/K-band SAA is carefully decided to be $D1 = 22$ mm ($0.7 \lambda_0$), and $D2 = 10$ mm ($0.7 \lambda_0$), respectively.

Parameter		X-band (9.65 GHz)		K-band (21 GHz)
		V-port	H-port	V-port
Bandwidth	MHz	9.65 GHz (10.36%)	9.65 GHz (10.36%)	21.027-21.040 (1.45%)
Gain	dBi	24	24.2	17.4
Radiation efficiency	%	85	85	82
E-plane	SLL (°)	-18.9	-19.2	-26.3
	HPBW (deg)	10.6	12.4	9.1
	Cross-pol (dB)	24	24	30
H-plane	SLL (dB)	-12.2	-11.3	-26
	HPBW (°)	12.4	10.6	64.9
	Cross-pol (dB)	23	22	25
Aperture area (A_p)		$150 \times 150 \times 1.6 \text{ mm}^3$		
Effective area (A_e)			$80 \times 80 \text{ mm}^2$	$10 \times 0.8 \text{ mm}^2$
Aperture efficiency (ϵ_a)			28.44%	0.44%

Notes: For X-band, one group is 24% for all four groups 24×4 , that is, 96%.

For K-band, the utilization effective area is 0.88%.

Efficient utilization of X/K-band SAA is 96.44%.

Abbreviations: HPBW, half-power beamwidth; SLL, side-lobe level.

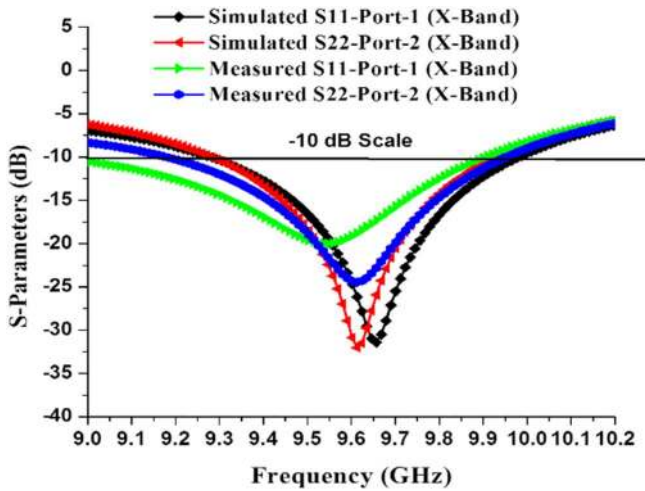


FIGURE 3 Simulated and measured scattering parameters of the X/K shared aperture antenna at X-band operation

Microstrip line feeding and coaxial probe feeding are used for X-band and K-band elements, and series feeding is used to feed the X/K-band SAA. RT/Duroid 5880 substrate with a relative dielectric constant of 2.2 and loss tangent of 0.0009 is used in the design [31]. The performance of these SAAs was analysed using the computer simulation technology microwave studio simulation software based on the finite integration technique [32]. The overall size of the X/K-band SAA is $150 \times 150 \times 1.6 \text{ mm}^3$. Another important task in SAA design is to accommodate the feed networks for both the bands for polarization diversity with compact in size. Generally, the feed networks for multi-frequencies are printed on separate layers. For the proposed SAA, however, we adopted series-fed

TABLE 3 Summary of X/K-band shared aperture antenna (SAA)

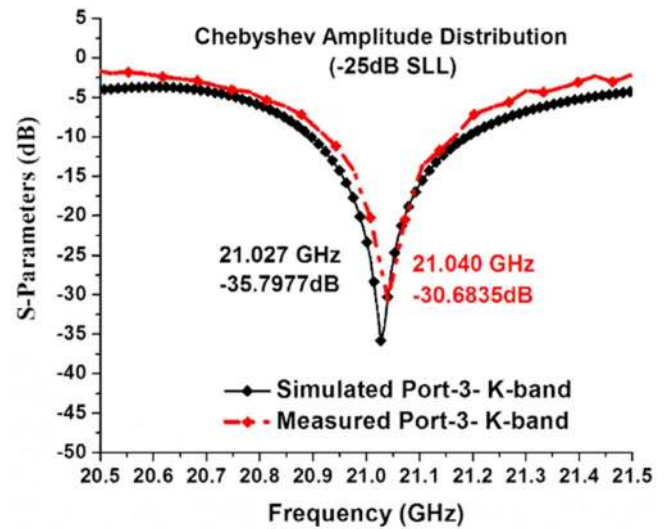


FIGURE 4 Simulated and measured scattering parameters of X/K-band shared aperture antenna at K-band operation

technology in the in-plane substrate, and external two-way and three-way power combiners/dividers are used along with radio frequency cables. Because of the high-frequency ratio between the X/K-bands, the two arrays with series feeding can be printed on the same plane. It is feasible to print the both arrays on the same plane with series feeding. This resulted in reduced complexity and costs in manufacturing.

To form arrays with higher gain, three kinds of external feed networks, X-band two-way power divider, X-band three-way power divider, and X-band hybrid coupler are applied in the system where higher gain with LP and circular polarization (CP) characteristics are needed, respectively. A prototype array

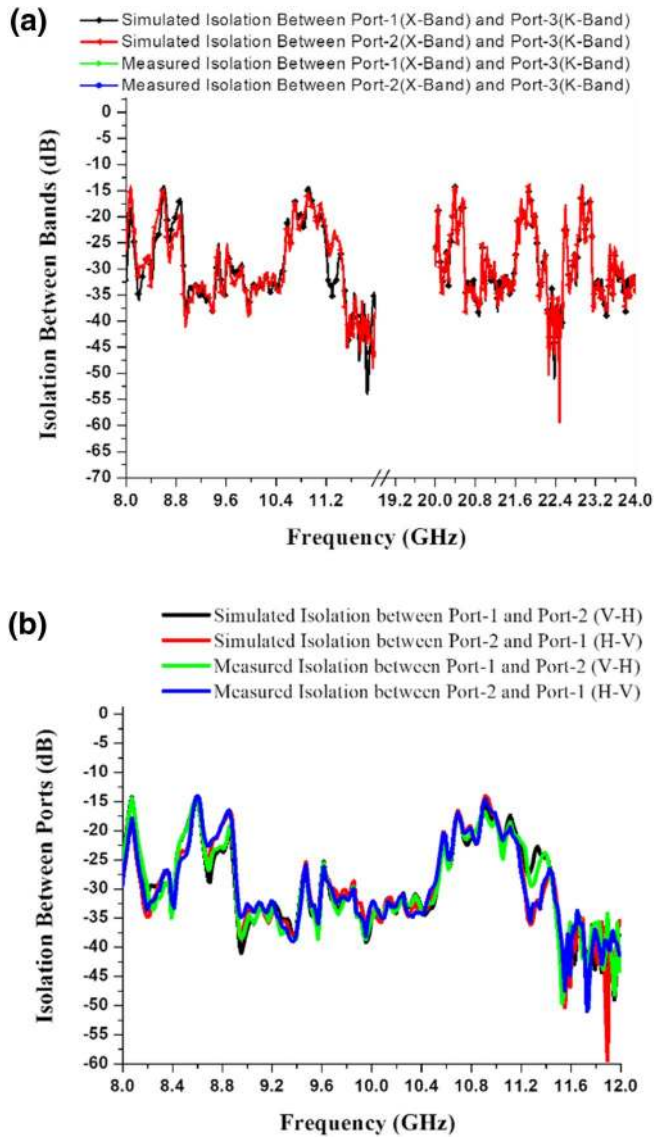


FIGURE 5 Simulated and measured scattering parameters (isolation) of the dual-band X/K shared aperture antenna array antenna: (a) Isolation between the ports; (b) isolation between the bands

with power dividers and hybrid coupler is fabricated and tested for both bands. The experimental results show that good CP characteristics are obtained. The 3-dB axial ratio (AR) bandwidth is around 14.2% for right-hand circular polarization (RHCP) and, left-hand circular polarization (LHCP) resonant at 9.65 GHz, respectively.

The geometry of the proposed X/K-band SAA with evolution stages are illustrated in Figure 2. The array consists of four groups of identical series-fed $3^\circ \times 3$ planar antenna array with element group mirroring in both vertical and horizontal planes has been implemented with vertical (V1, V2, and V3) and horizontal (H1, H2, and H3) ports for dual polarization shown as stage 1, Chebyshev K-band array shown as stage 2, the K-band co-axial probe feed is from the backside (ground plane) to the top of the proposed SAA, and finally, the K-band array elements have been accommodated in stage 3 are

represented with clear notations in Figure 1 as X/K-SAA. The element spacing employed in X/K-band array is of 0.7λ , which corresponds to resonant frequency 9.65 GHz (approximately one-guided wavelength), which is SFL (series-fed line) = 20 mm in this SAA X-band linear array. Optimum spacing has been selected to save the number of antenna elements for a narrow beam and good directivity. The element distance is limited by the beam scanning requirement. In X/K-band SAA, the element distance for square distribution can be decided in X- and Y-directions by Equations (1) and (2). These equations are inter-element spacing for both vertical and horizontal polarizations at X-band, that is, 9.65 GHz.

$$d_x = \frac{\lambda_V}{1 + \sin\theta_x} \quad (1)$$

$$d_y = \frac{\lambda_H}{1 + \sin\theta_y} \quad (2)$$

where λ_V and λ_H are the vertical and horizontal free-space wavelength of 9.65 GHz; d_x and d_y are the distances between the elements in X-direction and Y-directions; and θ_x and θ_y are the maximum scan angles of 25° .

Figure 1 shows the configuration of the 3×3 series fed, six-port planar array (Group 1). For X-band array design, S_{11} shows the best case quarter-wave transformer width (QWT = 0.28 mm); QTL = $2(\lambda_g = 24.57 \text{ mm}; \lambda_g/4 = 6.14 \text{ mm})$ with optimization for the resonant frequency of 9.65 GHz the value of quarter-wave transformer is 2 mm which is approximately $\lambda_g/10$ and QWT = 0.28 mm ($\approx 146 \Omega$). This impedance variation is because of the array environment. The effect of series feeding leads to impedance change in quarter-wave transformer ($\lambda_g/4$). The nine square patches (3×3) are connected to each other by series feeding in a 2-D method using the lines with dimensions of series-fed width (SFW) and SFL are 1.9 and 20 mm from the one patch feed point to another (Figure 1). To design a 0.7λ array in xz and yz planes, the value of SFL was selected to be 20 mm which provides a scan angle of $\pm 25^\circ$ in the elevation plane from the zenith angle of the upper hemisphere. To improve the impedance matching between the elements, the value of SFW was optimized to 1.9 mm ($\approx 59 \Omega$). Table 2 shows the dimensions of the designed prototype.

For K-band linear array design, Figure 1 shows the geometry of the Chebyshev amplitude distribution for the array. The antenna is composed of a microstrip patch array with an open-stub, series-fed, co-axial probe centre-feed (SFCFOS) structures. The optimized parameters are given in Table 3. In this K-band array, a Chebyshev characteristic of -25 dB relative SLL has been chosen. To achieve a flat SLL performance, the amplitude coefficients were modified from an ordinary Chebyshev synthesis and a half-wavelength open-ended stub was introduced after the last element for an effective use of transmitted energy. The centre patch width is 5 mm; the patch width of other elements varies with a ratio of 1, 0.9214, 0.778, 0.5944, and 0.6412 from the centre of the array to the edges. The distance between the two

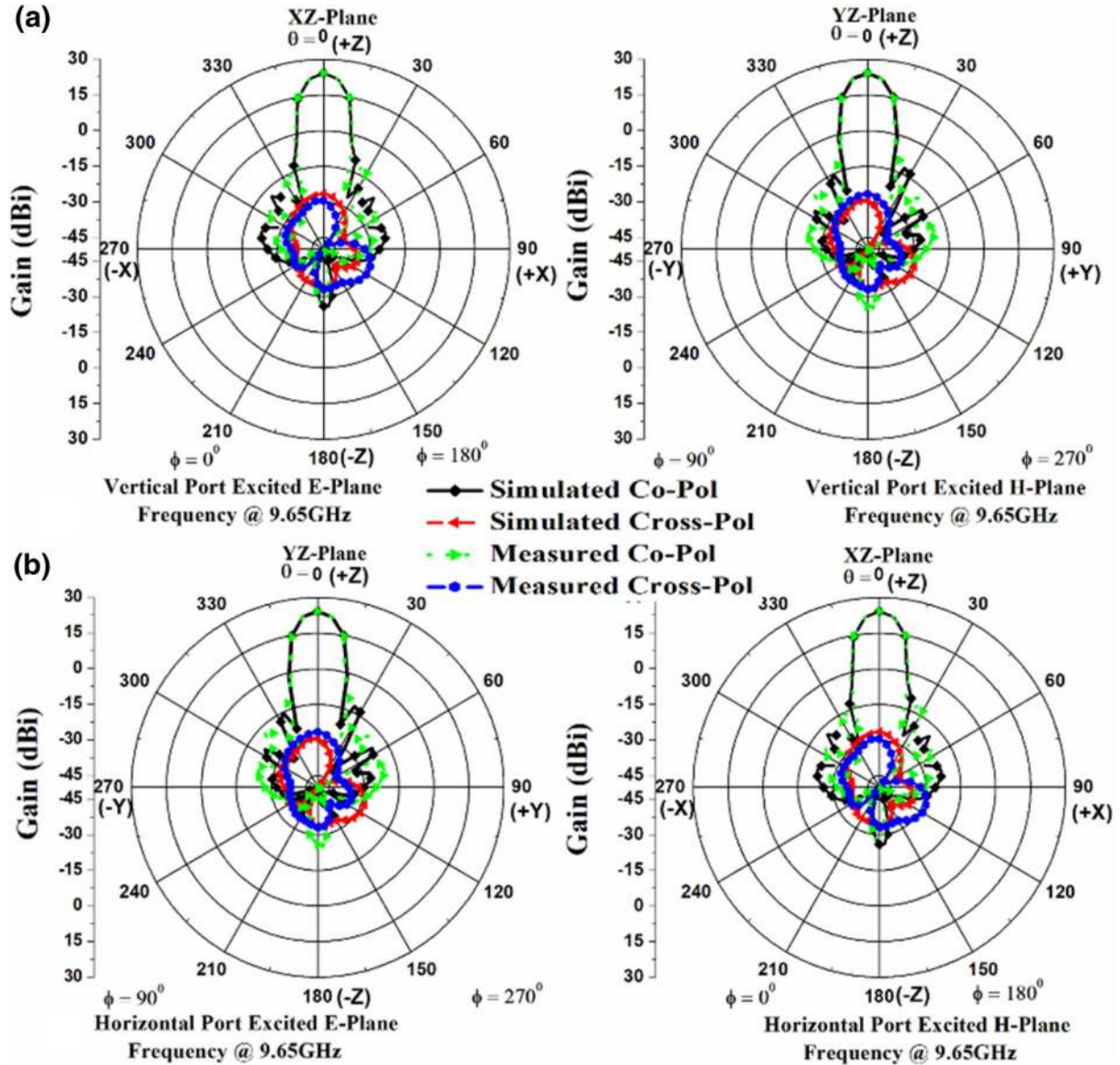


FIGURE 6 Simulated and measured radiation patterns of the X/K-band shared aperture antenna at 9.65 GHz: (a) V-port, Port-1 excitation; (b) H-port, Port-2 excitation

adjacent elements is 4.28 mm. The total size of the proposed Chebyshev linear array (CLA) antenna array is 100 mm (L), 15 mm (W), and 0.787 mm (H), respectively.

3 | RESULTS AND DISCUSSIONS

The X/K-band SAA is fabricated and experimentally verified. Figure 2 presents the SAA prototype measurement set-up and front view; Figure 2(b) presents the combined V- and H-ports with two-way and three-way power combiner/dividers for LP (both vertical and horizontal polarizations); and Figure 2(c) presents the SAA X/K-band array with externally connected hybrid coupler for CP (both LHCP/RHCP). The scattering parameters were measured with an Agilent N9918 A microwave analyser. Radiation characteristics and gain were measured with

Agilent PNA series network analyser N5230C (10 MHz–40 GHz) in an anechoic chamber (6 m \times 4 m \times 3 m ($L \times W \times H$)) with the standard gain horn as the reference antenna.

The simulated and experimentally measured S -parameters of the X-band array antenna is shown in Figures 3–5. The notation of P1 refers to the vertical port of the X-band and P2 refers to the horizontal port of the X-band and P3 refers to the port of the K-band. A good agreement between measured and simulated results was observed, with a fractional bandwidth (FBW) of -10 dB at port-1 (P1) and port-2 (P2) ranging from 9.2 to 10.1 GHz (FBW = 10.36%).

At K-band, the array has an impedance bandwidth ranging from 20.89 to 21.196 GHz (FBW = 1.45%) for the CLA as shown in Figure 4. The Chebyshev array has given -30.68 dB return loss port-3 (P3) at the centre frequency with gains of

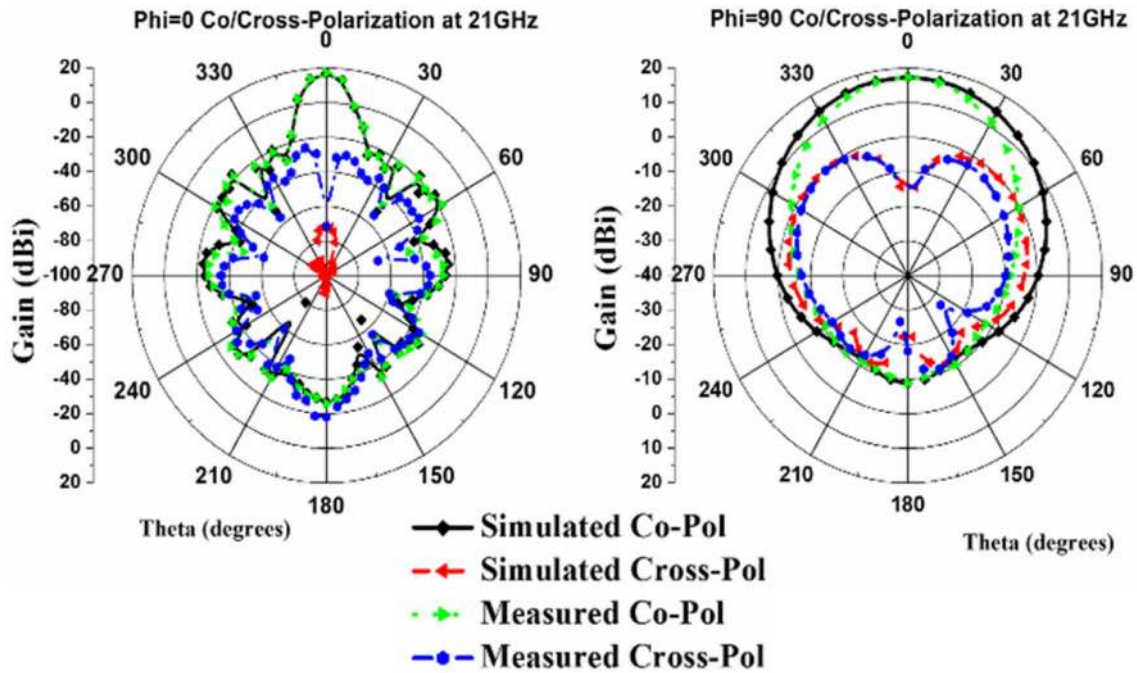


FIGURE 7 Simulated and measured radiation patterns of the X/K-band shared aperture antenna at 21 GHz (Port-3 excitation)

17.4 dBi. The results agree well with simulated and measured antenna parameters. Isolation higher than 25 in both X- and K-bands is obtained. Figure 5(a) gives the simulated and measured isolation results between X/K-bands. In addition, Figure 5(b) shows that the measured isolation between X/K bands is better than 25 dB in the same polarization and the isolation between X/K bands is better than 23 dB in two orthogonal ports.

Figure 6(a) shows the simulated and experimental radiation characteristics of the proposed X/K-band SAA at 9.65 GHz when P1 (X-band vertical port) is excited and P2 (X-band horizontal port) is terminated with a 50Ω matched loads. The measured results show the vertical polarized radiation characteristics. The measured X-pol is higher than 20 dB, and the measured side-lobe level (SLL) is less than -18.9 dB in E-plane and 23 dB (X-pol) and -12.2 dB (SLL) in H-plane.

Figure 6(b) shows the simulated and experimental radiation characteristics of the proposed X/K-band shared aperture antenna at 9.65 GHz when P2 (X-band horizontal port) is excited and P1 (X-band vertical port) and P3 (K-band) is terminated with a 50Ω matched load. The experimental results are in good agreement with the simulations, showing the horizontal polarization characteristics. The measured side-lobe levels are less than -19.2 and -11.3 dB and the measured X-pol levels are more than 24 dB in the E-plane and 22 dB in the H-plane. The gain at 9.65 GHz is 24.2 dBi and the radiation efficiency at both P1 and P2 is more than 85%.

Figure 7 shows the simulated and measured radiation patterns of the 10-element K-band SFCFOS array at 21 GHz. In the experiment, the SLLs are below 26 dB. The measured cross-pol is higher than 25 dB. The measured gain of SFCFOS array at 21 GHz is 17.4 dBi and the radiation

efficiency is about 82%. For the K-band design, the half-power beamwidth (HPBW) is $9.1^\circ/64.9^\circ$ for the E/H-planes. In addition, the maximum SLLs for the E- and H-planes are -26.3 and -26 dB, respectively.

The presented design can switch from LP to the LHCP and RHCP by extending the current design with a hybrid coupler at vertical and horizontal ports of the two-way power dividers as shown in Figure 1(c). The simulated and experimental radiation characteristics of the proposed X/K-band SAA at 9.65 GHz when LHCP-port is excited and RHCP-port and P3 (K-band) are terminated with a 50Ω matched load as shown in Figure 8(a).

The measured SLLs are less than -19.2 dB and X-pol levels are better than 24 dB in the E-plane and -11.3 and 22 dB in H-plane. The gain at 9.65 GHz is 24.2 dBi and the radiation efficiency is over 85% at both V- and H-ports and 17 dBi gain at 21 GHz K-band with 82% efficiency as shown in Figure 9.

At the designated frequency of 9.65 GHz, as shown in Figure 9(a), the measured gain is 24.2 dBic. When the X-band array with P1 is excited, the antenna has a gain of 24 dBic over impedance bandwidth. The measured gain at 9.65 GHz is 24.1 dBic and HPBW is 10.8° at E-plane and 12.6° at H-plane. The aperture efficiency of the antenna at the two ports is 85% and 87%, respectively.

Figure 10 shows the experimental and simulated X-band AR. When the LHCP/RHCP port is excited, the X-band array has a bandwidth of 3 dB AR from 8.6 to 10 GHz (14.5%). It has been observed that the bandwidths of the 3 dB AR are completely within the corresponding bandwidths of the two-port polarizations.

The measured gain of this X/K-band is high around 24/17 dBi. Since the gain of the proposed SAA design was high the

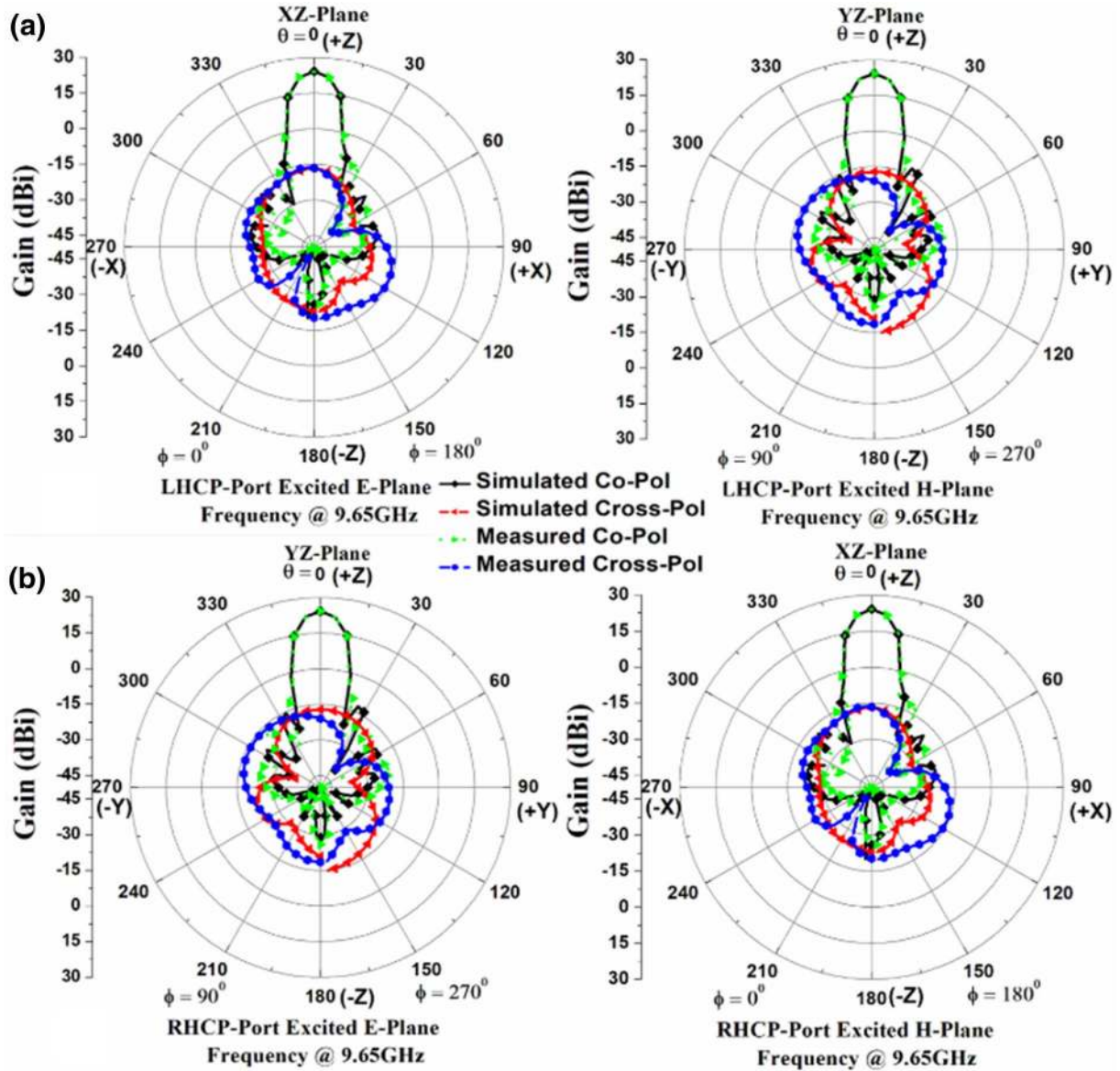


FIGURE 8 Simulated and measured radiation patterns of the X-band at 9.65 GHz: (a) left-hand circular polarization port excitation; (b) left-hand circular polarization port excitation

change in geometry between the antenna in flight and antenna in anechoic chamber error/loss will be very marginal.

So, change in the line-of-sight acquisition to the oblique acquisition will not be affected much. All the anechoic chamber measurements have been done in as per the well-established path. The distance between the transmitting antenna and receiving antennas are in the far-field region as follows [10]:

$$r > \frac{2D^2}{\lambda} \quad (3)$$

To prove the concept of shared aperture antenna using a single layer the prototype has been developed and achieved reasonable electrical (S -parameters) and radiation characteristics in comparison with simulated and measured results. The summary of X/K-band SAA has been given in Table 3.

Beam pointing variation with respect to frequency in the bandwidth is one of the major impediments in the phased array antenna. Pointing variation is attributed to constant phase shift applied to each radiator and it can be tolerated if in the range 5%–10% of the beam width [33]. SAA antenna designed herewith has shown bandwidth 10.36% and 25° of steering angle along the elevation plane, the pointing variation expected will be in the order of 2.59° for X-band. This value has to be compared with the antenna beamwidth 25° along that plane which is within the tolerable limit. Since, in this antenna design pointing variation is not large there is no need to introduce true-time delay lines in the beamformers as compared to conventional designs.

In this study, a solution is proposed to achieve a dual-band SAA of 2.176 frequency ratio (FR) in a single-layer microstrip patch antenna array. A 36-element X-band and 10-element K-band array prototypes are designed and fabricated. In contrast

to the antenna arrays presented in [22,28,30], the proposed SAA has a lower FR of 2.176. The proposed antenna array showed not only higher gains but also low SLLs in both bands compared to [21–26,28,30]. The small-FR dual-band prototype has a simple and convenient SAA design compared to [18,19]

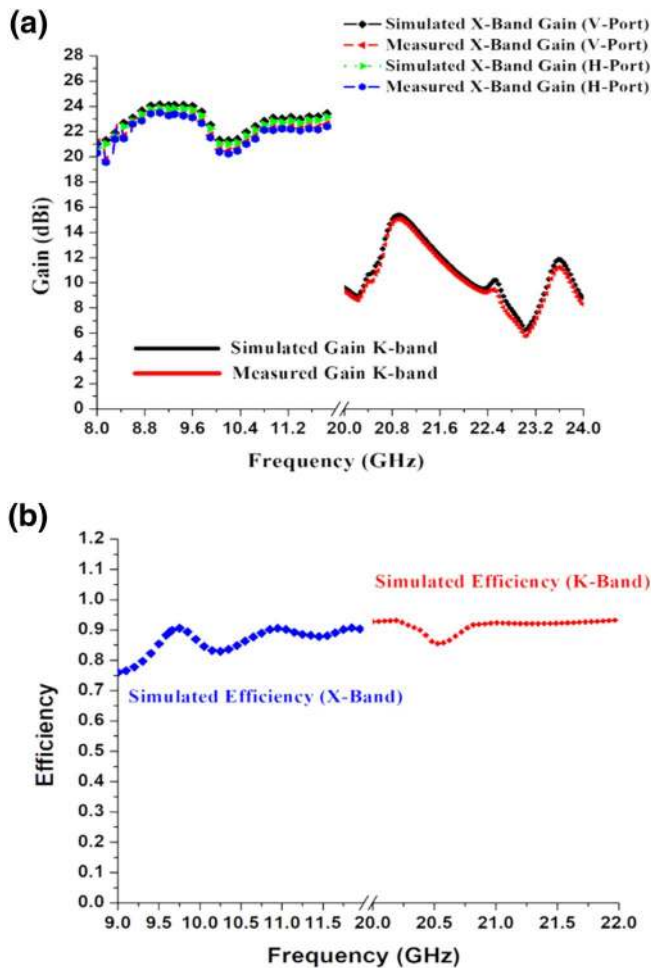


FIGURE 9 Simulated and measured gains and the simulated radiation efficiency of the X/K-band shared aperture antenna

and a low-profile, low-cost, single-layer, and planar configuration. Table 4 shows the proposed SAA in comparison with other SAAs. The prototype confirms a new SAA design with reasonable performance features.

4 | CONCLUSION

An SAA with X/K-band dual (linear or CP) polarized design with a single layer is presented for the first time. The square patch and width-controlled microstrip patch are taken as X/K-band elements for two arrays. To accommodate the K-band array within a common aperture, the Chebyshev technique (SFCFOS) with a width-controlled patch antenna is implemented. The feeding systems of the X/K-bands are etched on the same layer while maintaining the good isolation and X-pol levels. The present X/K-SAA is simulated, fabricated, and experimentally verified, showing a matching bandwidth of 10.36% (use of external power dividers and transmission line cables), and 1.45% at X/K-bands, respectively. Isolations

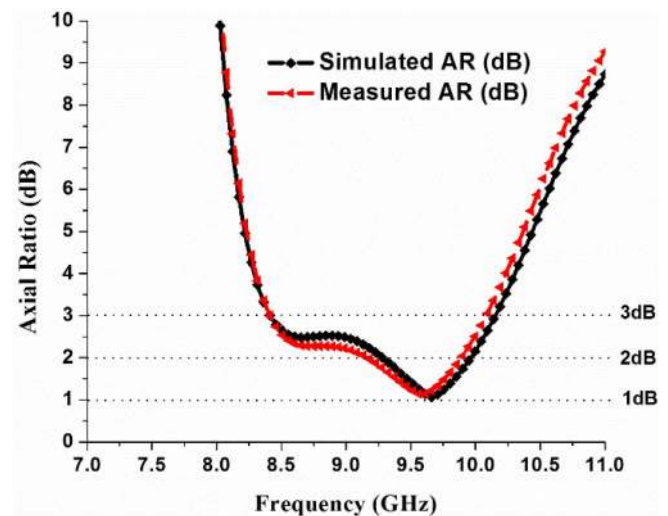


FIGURE 10 Simulated and measured axial ratio (dB) over frequency (X-band)

TABLE 4 Comparison with other shared aperture antenna


SAA	Year	Operation bands	Frequency ratio	Configuration	Gain (dBi)	SLL (dB)	Band 1/Band 2	Aperture size (mm)
[22]	2012	L/X (1.16/9.6)	8.275	Multilayer	11.1/23.5	-17.1/-11.1	NA	NA
[30]	2015	L/X (1.15/9.5)	8.26	Multilayer	6.9/21.4	NA/-10		240 × 240 × 27 mm ³
[21]	2016	K/KA (20/30)	1.5	Multilayer	4.4/4.6	NA/NA		NA
[23]	2016	C/X (5.3/9.6)	1.8	Multilayer	16.2/21.2	-10/-10		140 × 140 × 48 mm ³
[24]	2016	X/KU(12.2/17.5)	1.43	Single layer	17.45/18.26	-9/-10		71 × 64 × 0.762 mm ³
[28]	2017	S/X (3.2/9.3)	2.906	Single layer	8.5/11	-17/-20		100 × 100 × 1.6 mm ³
[25]	2017	C/X (5.3/8.2)	1.54	Multilayer	14.5/17.5	-12.5/-15		110 × 110 × 4.6 mm ³
[26]	2018	K/KA (13.5/24)	1.77	Multilayer	11/14.4	NA/NA		64 × 53 × 7 mm ³
This work		X/K (9.65/21)	2.176	Single layer	24/17.2	-15/-26		150 × 150 × 1.6 mm ³

between P1, P2, and P3 polarizations in X/K-bands are more than 25 dB. The presented X/K-SAA also has excellent SLL, gain, efficiency, and X-pol radiation performance. The dimensions of the X/K-band SAA are in compact and occupy an area of $150 \times 150 \times 1.6 \text{ mm}^3$. The prototype of SAA design showed compactness, less cost, easy to model, and single-layer structure, and thus suited for large-size SAA for the ASAR systems. Due to cost constraints and limited facilities available, the authors fabricated the prototype with the minimum number of elements for the proof of concept and achieved reasonable electrical (S -parameters) and radiation characteristics in comparison with simulated and measured results. In the future, this SAA can be extended to large arrays for meeting the requirements of ASAR.

ACKNOWLEDGEMENT

This work is supported by the DST-SERB Government of India, grant with Ref. No.SB/DGH-82/2014. The work has been done at Microwave Division, School of Electronics Engineering (SENSE), Vellore Institute of Technology (VIT), Vellore, Tamil Nadu, India. All the assistance provided by the department and university administration to carry out this work is highly appreciated.

ORCID

Venkata Kishore Kothapudi  <https://orcid.org/0000-0002-6247-5461>

Vijay Kumar  <https://orcid.org/0000-0001-8738-8404>

REFERENCES

- Skolnik, M.I.: Radar Handbook, 3rd edn, pp. 1.1–24.1. McGraw-Hill, New York (1970). <https://www.accessengineeringlibrary.com/content/book/9780071485470>
- Drinkwater, M.R., Kwok, R., Rignot, E.: Synthetic aperture radar polarimetry of sea ice. In: Digest—International Geoscience and Remote Sensing Symposium (IGARSS), Vol. 2, pp. 1525–1528 (1990)
- Lynne, G.J., Taylor, G.R.: Geological assessment of SIRB imagery of the Amadeus basin, N.T., Australia. *IEEE Trans. Geosci. Remote Sens.* 24(4), 575–581 (1986)
- Hovland, H.A., Johannessen, J.A., Digranes, G.: Slick detection in SAR images. In: International Geoscience and Remote Sensing Symposium (IGARSS), Vol. 4, pp. 2038–2040 (1994)
- Walker, B., et al.: High-resolution, four-band SAR testbed with real-time image formation. In: International Geoscience and Remote Sensing Symposium (IGARSS), Vol. 3, pp. 1881–1885 (1996)
- Storvold, R., et al.: SAR remote sensing of snow parameters in Norwegian areas—current status and future perspective. *J. Electromagn. Waves Appl.* 20(13), 1751–1759 (2006)
- Kong, J.A., et al.: Classification of earth terrain using polarimetric synthetic aperture radar images. *PIER, Progress In Electromagnetic Research.* 327–370 (1990). <http://www.jpier.org/PIER/pier03/06.900101.pdf>
- Jordan, R.L., Huneycutt, B. L., Werner, M.: The SIR-C/X-SAR synthetic aperture radar system. *IEEE Trans. Geosci. Remote Sens.* 33(4), 829–839 (1995)
- Axness, T.A., et al.: Shared aperture technology development. *Johns Hopkins APL Tech Dig.* 17(3), 285–293 (1996)
- Balanis, C.A.: Antenna theory: Analysis and design. *Antennas & Propagation.* 4th edn. Wiley, Hoboken (1997)
- Shafai, L.L., et al.: Dual-band dual-polarized perforated microstrip antennas for SAR applications. *IEEE Trans. Antenn. Propag.* 48(1), 58–66 (2000)
- Pozar, D.M., Targonski, S.D.: A shared-aperture dual-band dual-polarized microstrip array. *IEEE Trans. Antenn. Propag.* 49(2), 150–157 (2001)
- Chiou, T.-W., Wong, K.-L.: A compact dual-band dual-polarized patch antenna for 900/1800-MHz cellular systems. *IEEE Trans. Antenn. Propag.* 51(8), 1936–1940 (2003)
- Vetharatnam, G., Kuan, C.B., Teik, C.H.: Combined feed network for a shared-aperture dual-band dual-polarized array. *IEEE Antenn. Wirel. Propag. Lett.* 4, 297–299 (2005)
- Soodmand, S.: A novel circular-shaped dual-band dual-polarized patch antenna and introducing a new approach for designing combined feed networks. In: The Loughborough Antennas Propagation Conference (LAPC), pp. 401–404 (2009)
- Pokuls, R., Uher, J., Pozar, D.M.: Microstrip antennas for SAR applications. *IEEE Trans. Antenn. Propag.* 46(9), 1289–1296 (1998)
- Yang, Z., Warnick, K.F.: Multiband dual-polarization high-efficiency array feed for Ku/reverse-band satellite communications. *IEEE Antenn. Wirel. Propag.* 13, 1325–1328 (2014)
- Moghadas, H., Daneshmand, M., Mousavi, P.: A dual-band high-gain resonant cavity antenna with orthogonal polarizations. *IEEE Antenn. Wirel. Propag.* 10, 1220–1223 (2011)
- Naishadham, K., et al.: A shared-aperture dual-band planar array with self-similar printed folded dipoles. *IEEE Trans. Antenn. Propag.* 61(2), 606–613 (2013)
- Zhon, S.-S., et al.: Tri-band dual-polarization shared-aperture microstrip array for SAR applications. *IEEE Trans. Antenn. Propag.* 60(9), 4157–4165 (2012)
- Sandhu, I., et al.: Radiating elements for shared aperture Tx/Rx phased arrays at K/Ka-Band. *IEEE Trans. Antenn. Propag.* 64(6), 2270–2282 (2016)
- Gang, Z.S., Huat, C.T., Jian, L.: A shared-aperture dual-wideband dual-polarized stacked microstrip array. *Microw. Opt. Technol. Lett.* 54(2), 486–491 (2012)
- Qin, F., et al.: A simple low-cost shared-aperture dual-band dual-polarized high-gain antenna for synthetic aperture radars. *IEEE Trans. Antenn. Propag.* 64(7), 2914–2922 (2016)
- Zhang, J.-D., Wu, W., Fang, D.-G.: Dual-band and dual-circularly polarized shared-aperture array antennas with the single-layer substrate. *IEEE Trans. Antenn. Propag.* 64(1), 109–116 (2016)
- Mao, C.-X., et al.: Dual-band circularly polarized shared-aperture array for C-/X-band satellite communications. *IEEE Trans. Antenn. Propag.* 65(10), 5171–5178 (2017)
- Li, M., et al.: Triband planar shared-aperture antenna array with similarly shaped radiation patterns. *Microw. Opt. Technol. Lett.* 60(9), 2284–2294 (2018)
- Mao, C., et al.: Low-cost X/Ku/Ka-Band dual-polarized array with shared aperture. *IEEE Trans. Antenn. Propag.* 65(7), 3520–3527 (2017)
- Kothapudi, V.K., Kumar, V.: A single layer S/X-band series-fed shared aperture antenna for SAR applications. *Progr. Electromagn. Res. C.* 76, 207–219 (2017)
- Kothapudi, V.K., Kumar, V.: A 6-port two-dimensional 3×3 series-fed planar array antenna for dual-polarized X-band Airborne synthetic aperture radar applications. *IEEE Access.* 6, 12001–12007 (2018)
- Zhou, S.-G., Yang, J.-J., Chio, T.-H.: Design of L/X-band shared aperture antenna array for SAR application. *Microw. Opt. Technol. Lett.* 57(9), 2197–2204 (2015)
- Rogers Corporation. www.rogerscorp.com
- Computer Simulation Technology Version, Wellesley Hills, MA. www.cst.com (2016)
- Capece, P.: Active SAR antennas: design, development, and current programs. *Int. J. Antenn. Propag.* 2009, 796064 (2009)

How to cite this article: Kothapudi VK, Kumar V. Hybrid-fed shared aperture antenna array for X/K-band airborne synthetic aperture radar applications. *IET Microw. Antennas Propag.* 2021;15:93–102. <https://doi.org/10.1049/mia2.12024>